Molecular Therapy
Nucleic Acids
Original Article

miR-374a-5p: A New Target for Diagnosis and Drug Resistance Therapy in Gastric Cancer

Runbi Ji,[1] Xu Zhang,[2] Hongbing Gu,[1] Jichun Ma,[1] Xiangmei Wen,[1] Jingdong Zhou,[1] Hui Qian,[2] Wenrong Xu,[2] Jun Qian,[1] and Jiang Lin[1]

[1]The Affiliated People's Hospital of Jiangsu University, Zhenjiang 212002, Jiangsu, China; [2]Jiangsu Key Laboratory of Medical Science and Laboratory Medicine, School of Medicine, Jiangsu University, Zhenjiang 212013, Jiangsu, China

Chemoresistance is one of the causes associated with poor prognosis in gastric cancer. MicroRNAs (miRNAs) are important regulators of chemoresistance. Exosome-mediated delivery of anti-cancer molecules and drugs have emerged as a new approach for cancer therapy. We first examined the expression of miR-374a-5p in gastric cancer serum by qRT-PCR and explored the clinicopathological parameters. We then performed *in vitro* cell and molecular studies, including CCK-8 assay, flow cytometry, qRT-PCR, and western blot, to determine the roles of miR-374a-5p in gastric cancer chemoresistance and identified its downstream target by luciferase reporter assay. We also used *in vivo* animal studies to evaluate the therapeutic efficacy of miR-374a-5p inhibitor and exosome-mediated delivery of miR-374a-5p inhibitor in gastric cancer. miR-374a-5p expression level was elevated in gastric cancer serum, and its upregulation predicted poor prognosis. miR-374a-5p overexpression promoted while miR-374a-5p knockdown inhibited gastric cancer chemoresistance *in vitro* and *in vivo*. miR-374a-5p bound to Neurod1 to antagonize its effect on chemoresistance. Exosome-mediated delivery of miR-374a-5p inhibitor could increase Neurod1 expression, promote cell apoptosis, and suppress chemoresistance. miR-374a-5p had a promoting role in gastric cancer chemoresistance, which would provide a novel biomarker for gastric cancer diagnosis and prognosis and offer a potential target for gastric cancer drug resistance therapy.

INTRODUCTION

Gastric cancer is one of the most common malignancies worldwide. On the one hand, most gastric cancer patients are diagnosed at advanced stages due to a lack of typical early symptoms. On the other hand, the patients often have a poor prognosis as a result of drug resistance.[1] Though great efforts have been made to understand the molecular mechanisms for gastric cancer development and progression, it is still a great challenge to identify novel targets for gastric cancer detection and treatment.

MicroRNAs (miRNAs) are important regulators of gene expression. We previously reported that miR-374a-5p was highly expressed in gastric cancer tissues compared with corresponding non-cancerous tissues by microarray screening.[2] Our recent study revealed that miR-374 promoted the proliferation and migration of transformed mesenchymal stem cells (MSCs) by regulating the Wnt5a/β-catenin signaling pathway, which, to a certain extent, contributed to the transformation of rat bone marrow-derived MSCs to the K3 tumor cell line.[3] In addition, the upregulation of miR-374 in MSCs from the gastritis tissues of MNNG (N-methyl-N′-nitro-N-nitrosoguanidine)-exposed rats could increase their proliferation and migration abilities.[4] Other studies showed that miR-374-5p overexpression promoted the proliferation, migration, and invasion of gastric cancer cells by targeting SRCIN1 and RECK genes.[5,6] All together, these findings suggest that miR-374a-5p is critically involved in the pathogenesis of gastric cancer and may be utilized as a target for gastric cancer diagnosis and treatment. However, there are few reports about the roles of miR-374a-5p in the drug resistance of gastric cancer.

Oxaliplatin, a first-line chemotherapeutic drug for gastric cancer, has synergistic effect when it is combined with 5-fluorouracil (5-FU).[7] We found that the expression of miR-374a-5p was raised in the serum of relapsed gastric cancer patients receiving oxaliplatin chemotherapy and oxaliplatin-pretreated gastric cancer cells. We thus hypothesized that miR-374a-5p might play a role in the drug resistance of gastric cancer.

miRNAs can be stably encapsulated in exosomes, small vesicles of endocytic origin. Exosomes regulate the phenotype and function of target cells by delivering genetic materials including miRNAs.[8–10] As a result of their high drug delivery efficiency and low toxicity and immunogenicity *in vivo*, exosomes have become a new vehicle for drug loading in cancer therapy.[11–13] Whether exosomes loaded with miR-374a-5p inhibitor could reverse chemoresistance in gastric cancer is not clear.

Received 21 February 2019; accepted 17 July 2019;
https://doi.org/10.1016/j.omtn.2019.07.025.

Correspondence: Jiang Lin, The Affiliated People's Hospital of Jiangsu University, 8 Dianli Road, Zhenjiang 212002, Jiangsu, China.
E-mail: 2651329493@qq.com
Correspondence: Xu Zhang, Jiangsu Key Laboratory of Medical Science and Laboratory Medicine, School of Medicine, Jiangsu University, 301 Xuefu Road, 212013, Jiangsu, China.
E-mail: xuzhang@ujs.edu.cn

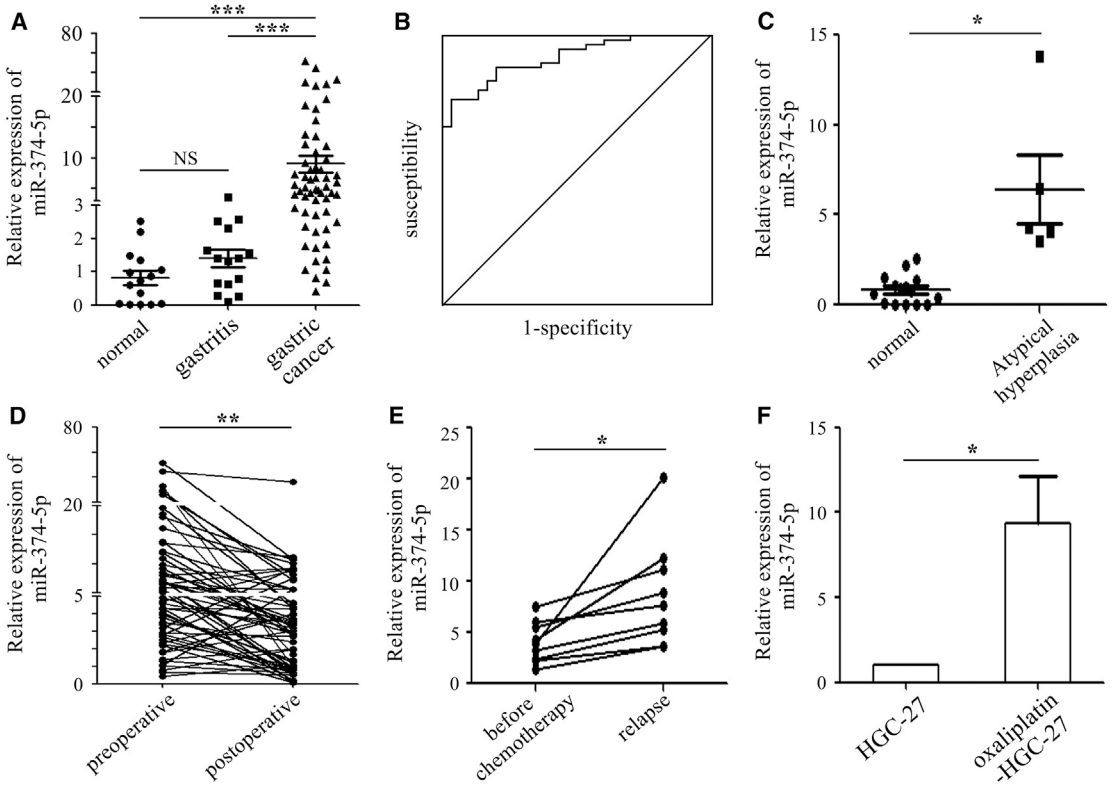

Figure 1. miR-374a-5p Is a Potential Diagnostic and Prognostic Marker for Gastric Cancer

(A) qRT-PCR analyses of miR-374a-5p expression in the serum of patients with gastric cancer (n = 59), gastritis (n = 17), and healthy controls (n = 17). (B) ROC curve for the diagnostic value of miR-374a-5p in the serum of gastric cancer patients. (C) qRT-PCR analyses of miR-374a-5p expression in the serum of patients with gastric pre-cancerous lesion (n = 5) and healthy controls (n = 17). (D) qRT-PCR analyses of miR-374a-5p expression in paired serum samples from pre-operative and post-operative patients (n = 59). (E) Comparison of miR-374a-5p expression levels in paired serum samples from gastric cancer patients that have not received chemotherapy and have relapsed after chemotherapy (n = 9) by qRT-PCR. (F) qRT-PCR analyses of miR-374a-5p expression in HGC-27 cells and oxaliplatin-resistant HGC-27 cells (oxaliplatin-HGC-27). *p < 0.05; **p < 0.01; ***p < 0.001.

In this study, we assessed miR-374a-5p expression in the serum of gastric cancer patients and explored the effects of miR-374a-5p on drug resistance in gastric cancer cells. We found that miR-374a-5p was upregulated in the serum of gastric cancer patients, and its high level was associated with gastric cancer progression and predicted poor prognosis. miR-374a-5p overexpression conferred chemoresistance of gastric cancer cells to oxaliplatin, and miR-374a-5p inhibitor-loading exosomes were capable of reversing oxaliplatin resistance both *in vitro* and *in vivo*. Our findings provide a potential biomarker for gastric cancer diagnosis and prognosis as well as a possible therapy approach for gastric cancer patients who are refractory to oxaliplatin.

RESULTS

miR-374a-5p Is Highly Expressed in the Serum of Gastric Cancer Patients, and a High Level of miR-374a-5p Is Associated with Poor Prognosis

We first detected the expression level of miR-374a-5p in the serum of patients with gastric cancer. The serum level of miR-374a-5p was elevated in gastric cancer patients compared to gastritis patients and healthy controls (Figure 1A). Combined with the clinicopathological characteristics analysis, we found that the expression level of miR-374a-5p in serum was higher in the group of tumors with a diameter greater than 5 cm compared to tumors with a diameter less than 5 cm. However, the miR-374a-5p expression had no relationship with other clinicopathological parameters (Table 1). Patients with gastritis and healthy persons were taken as control group (34 cases), and patients with gastric cancer as disease group (59 cases). The area under the receiver operating characteristic (ROC) curve for miR-374a-5p was 0.919, with 95% confidence interval (CI) 0.866 to 0.972 (Figure 1B). We next examined the expression level of miR-374a-5p in the serum of patients with pre-cancerous lesion confirmed by gastroscopy and pathology. The expression level of miR-374a-5p in the serum of patients with pre-cancerous lesions was about 5-fold higher than that in healthy controls (Figure 1C). We then measured the expression levels of miR-374a-5p in paired pre-operative and post-operative serum samples. As shown in Figure 1D, the expression level of circulating miR-374a-5p was notably reduced in the post-operative group compared to the pre-operative group. Additionally, miR-374a-5p expression level in the relapsed group

Table 1. The Association of Relative miR-374a-5p Expression Level with the Clinicopathological Characteristics of Gastric Cancer Patients

Characteristics	Number	No. of Patients		p Value
		miR-374a-5phigh	miR-374a-5plow	
Age (Years)				
>60	48	38	10	0.693
≤60	11	8	3	
Gender				
Male	41	34	7	0.187
Female	18	12	6	
Tumor Size (cm)				
≥5	29	27	2	0.010*
<5	30	19	11	
T Classification				
T1∼T2	11	9	2	1.000
T3∼T4	48	37	11	
N Classification				
N0	15	13	2	0.482
N1∼N3	44	33	11	
Involvement of Nerves and Blood Vessels				
Yes	9	7	2	1.000
No	50	39	11	

*p < 0.05.

was significantly higher than that in the before-chemotherapy group (Figure 1E). We also found that the expression level of miR-374a-5p also significantly raised in oxaliplatin-resistant HGC-27 cells compared with the parental cells (Figure 1F). Together, these findings suggested that miR-374a-5p might be involved in chemoresistance in gastric cancer.

miR-374a-5p Confers Drug Resistance of Gastric Cancer Cells *In Vitro* and *In Vivo*

We next studied the function of miR-374a-5p in gastric cancer chemoresistance. miR-374a-5p transfection in HGC-27 cells led to increased half-inhibitory concentration (IC_{50}) to oxaliplatin (18.24 ± 1.84 μg/mL) compared to untransfected cells (10.69 ± 0.88 μg/mL) (Figure 2A). Consistently, miR-374a-5p transfection also enhanced the IC_{50} of HGC-27 cells to 5-FU (Figure S1). The IC_{50} to oxaliplatin and 5-FU, in SGC-7901 and MGC-803 cells, was also increased by miR-374a-5p (Figure S1). Overexpression of miR-374a-5p upregulated the expression of multi-drug resistant (MDR) and topoisomerase II (Topo II) (Figures 2B and 2C). The apoptotic rate in the miR-374a-5p transfection group (8.82% ± 0.41%) was significantly lower than that in the control group (14.46% ± 3.14%) as detected by Annexin V-PE/7-aminoactinomycin D (7-AAD) apoptosis staining (Figure 2D). We then generated xenograft tumor models to validate our previous results. As indicated, agomir-374a-5p significantly promoted xenograft tumor growth following oxaliplatin treatment (Figure 2E). Tumor growth in the agomir-374a-5p group was faster than that in oxaliplatin alone and negative control groups. The mean tumor size in agomir-374a-5p group was about 380 mm^3 at the seventh day after chemotherapy, almost two times larger than that in oxaliplatin alone and negative control groups (Figure 2F). The mean tumor weight in the agomir-374a-5p group (0.62 ± 0.15 g) was approximately two times heavier than that in the oxaliplatin alone group (0.38 ± 0.06 g) (Figure 2G). Immunohistochemical analysis showed that tumor tissues from the agomir-374a-5p group displayed more positivity for MDR and Topo II than that in other groups (Figure 2H). The results of TUNEL staining demonstrated that co-treatment with agomir-374a-5p reduced the percentage of apoptotic cells *in vivo* (Figure 2I).

Knockdown of miR-374a-5p Re-sensitizes Oxaliplatin-HGC-27 Cells to Oxaliplatin *In Vitro* and *In Vivo*

We next depleted miR-374a-5p expression in oxaliplatin-HGC-27 cells (with increased expression of miR-374a-5p) by using miRNA inhibitor. Knockdown of miR-374a-5p resulted in a decreased IC_{50} to oxaliplatin in oxaliplatin-HGC-27 cells (12.23 ± 0.59 μg/mL) compared to control cells (18.65 ± 1.48 μg/mL) (Figure 3A). miR-374a-5p knockdown also reduced the expression of MDR and Topo II in oxaliplatin-HGC-27 cells (Figures 3B and 3C). The flow cytometry analyses revealed that knockdown of miR-374a-5p obviously induced cell apoptosis (9.42% ± 0.85%) compared to control group (4.69% ± 0.24%) (Figure 3D). Antagomir-374a-5p further inhibited tumor growth in oxaliplatin treatment group (Figure 3E). The mean tumor size and weight in the antagomir-374a-5p group were approximately half of that in oxaliplatin alone and negative control groups (Figures 3F and 3G). The results of immunohistochemical staining showed that the expression of MDR and Topo II proteins in antagomir-374a-5p group were lower than that in control group, whereas the results of TUNEL assay demonstrated an increase in the percentage of apoptotic cells in the antagomir-374a-5p group (Figures 3H and 3I). Taken together, our findings implied that miR-374a-5p was an important regulator of chemotherapy resistance in gastric cancer.

miR-374a-5p Promotes Drug Resistance by Targeting Neurod1 in Gastric Cancer

We next wanted to know the mechanism for the role of miR-374a-5p in drug resistance in gastric cancer. We identified neuronal differentiation 1 (Neurod1) as a potential target of miR-374a-5p by bioinformatic algorithms including miRTarBase, TargetScan, and miRGen software. To confirm the regulation of Neurod1 by miR-374a-5p, we constructed the corresponding wild-type (WT) reporter vector that contained the predicted binding sequence in the 3′ UTR of Neurod1 (Figure 4A). We performed luciferase assay for HGC-27 or oxaliplatin-HGC-27 cells that had been co-transfected with miR-374a-5p mimics (or inhibitor) and the WT (or mutant) luciferase reporter vector, respectively. The relative luciferase activity of Neurod1 was significantly decreased in miR-374a-5p mimic-transfected HGC-27 cells (Figure 4B), but the activity was elevated in miR-374a-5p inhibitor-transfected oxaliplatin-HGC-27 cells (Figure 4B). However,

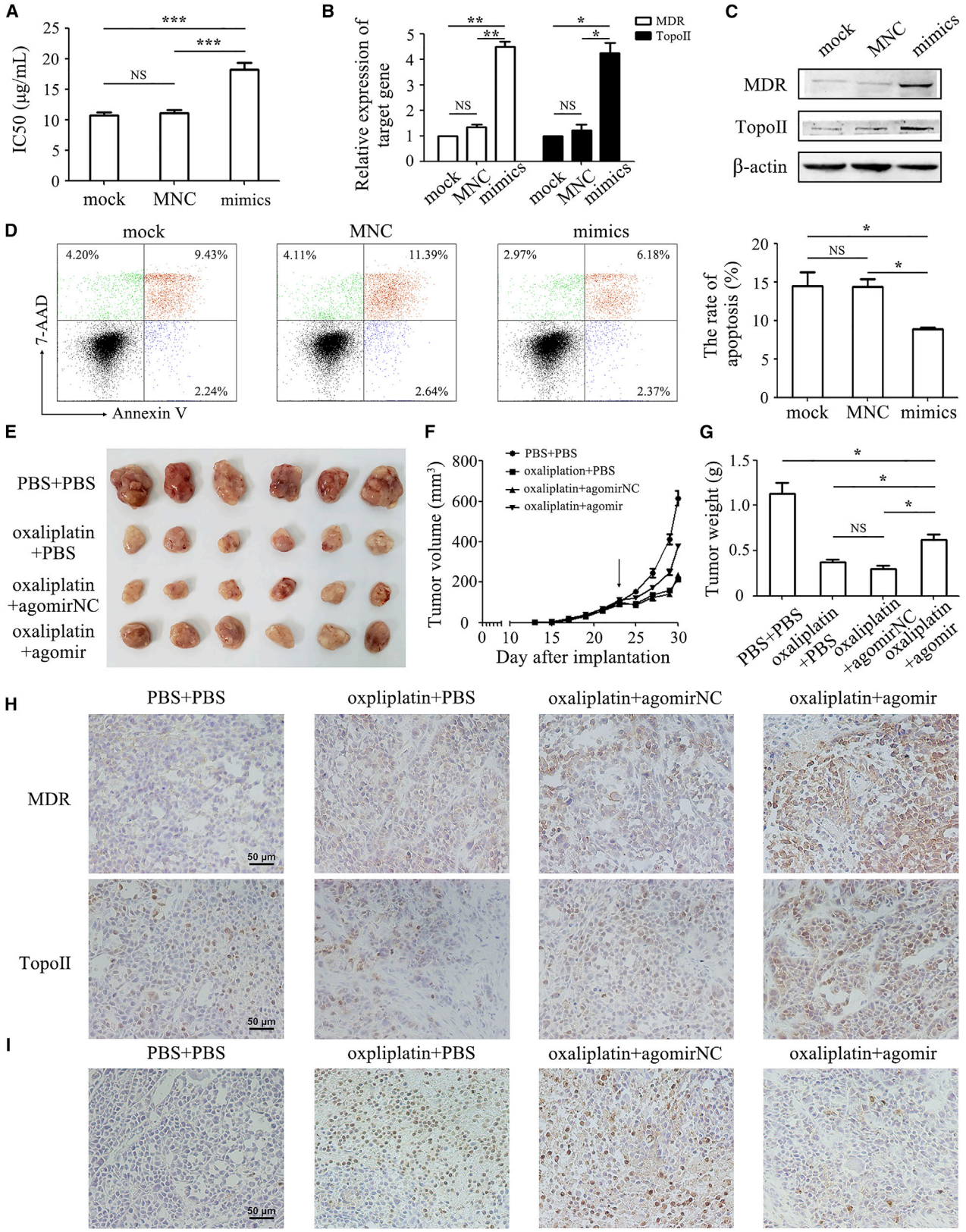

(legend on next page)

these changes were not observed when the predicted sites were mutated (Figures 4A and 4B). Meanwhile, miR-374a-5p overexpression decreased while miR-374a-5p knockdown increased Neurod1 expression at both mRNA and protein levels (Figures 4C and 4D). Moreover, the results of immunohistochemical analyses indicated that Neurod1 expression was downregulated in tumor tissues of the agomir-374a-5p group while upregulated in that of the antagomir-374a-5p group (Figure 4E). In summary, these results suggested that Neurod1 was a downstream target of miR-374a-5p.

Neurod1 Reverses miR-374a-5p-Mediated Drug Resistance in Gastric Cancer

We further validated the importance of Neurod1 inhibition by miR-374a-5p to drug resistance in gastric cancer. We co-transfected Neurod1 plasmid with miR-374a-5p mimics or Neurod1 small interfering RNA (siRNA) with miR-374a-5p inhibitor in HGC-27 or oxaliplatin-HGC-27 cells. Neurod1 overexpression reduced the IC_{50} of HGC-27 cells to oxaliplatin and re-sensitized miR-374a-5p-transfected HGC-27 cells to oxaliplatin (Figure 5A). On the contrary, Neurod1 knockdown increased the IC_{50} of oxaliplatin-HGC-27 cells to oxaliplatin and antagonized miR-374a-5p inhibitor-mediated re-sensitization of oxaliplatin-HGC-27 cells to oxaliplatin (Figure 5B). Neurod1 overexpression reversed the induction of MDR and Topo II protein expression by miR-374a-5p in HGC-27 cells, while Neurod1 knockdown increased the expression of MDR and Topo II proteins that had been reduced by miR-374a-5p inhibitor in oxaliplatin-HGC-27 cells (Figures 5C and 5D). Moreover, Neurod1 overexpression increased the percentage of apoptotic cells compared to control cells and also reversed the inhibition of cell apoptosis by miR-374a-5p mimics in HGC-27 cells (Figure 5E). However, Neurod1 knockdown decreased the percentage of apoptotic cells and antagonized the induced apoptosis by miR-374a-5p inhibitor in oxaliplatin-HGC-27 cells (Figure 5F).

Exosome-Mediated Delivery of miR-374a-5p Inhibitor Reverses Drug Resistance in Gastric Cancer *In Vitro* and *In Vivo*

We next wanted to test whether exosomes could deliver anti-miR-374a-5p into cells and exerted the above-mentioned effects in gastric cancer cells. We isolated exosomes from HEK293T cells that had been transfected with inhibitor of miR-374a-5p (anti-miR-374a-5p) and negative control. These exosomes were small, round vesicles with a diameter ranging from 40 to 100 nm (Figure S2A), expressed the exosomal markers CD63 and CD9 (Figure S2B), and could be internalized by HGC-27 (Figure S2C). We found that the level of miR-374a-5p was lower in exosomes from the anti-miR-374a-5p group than that in exosomes from the negative control group (Figure S2D). The expression level of anti-miR-374a-5p was remarkably upregulated in exosomes from the anti-miR-374a-5p group compared to the negative control group (Figure S2E). Similar to that observed for miR-374a-5p inhibitor transfection, exosome-mediated delivery of anti-miR-374a-5p (exo-anti-374a-5p) could also upregulate the expression of Neurod1 in oxaliplatin-HGC-27 cells (Figures 6A and 6C). The IC_{50} of oxaliplatin-HGC-27 cells to oxaliplatin was decreased by exo-anti-374a-5p (Figure 6B). The expression of MDR and Topo II in oxaliplatin-HGC-27 cells was decreased by exo-anti-374a-5p (Figure 6C). Additionally, exo-anti-374a-5p induced cell apoptosis in oxaliplatin-HGC-27 cells (Figure 6D). Subsequently, the intratumoral injection of exo-anti-374a-5p led to significant inhibition of tumor growth when combined with oxaliplatin treatment (Figure 6E). Compared to that in the oxaliplatin-alone treatment group, the tumors in the exo-anti-374a-5p group had smaller size (Figure 6F) and lighter weight (Figure 6G). The expression level of miR-374a-5p in tumor tissues was downregulated by exo-anti-374a-5p (Figure 6H). The results of immunohistochemical analyses showed that the expression of Neurod1 was upregulated, while that of MDR and Topo II was downregulated in tumor tissues from exo-anti-374a-5p group compared to the negative control group (Figure 6I). Moreover, the number of apoptotic cells was increased in the exo-anti-374a-5p group compared to the negative control group (Figure 6J). Therefore, these findings suggested that exo-anti-374a-5p might be a potential approach for drug resistance therapy in gastric cancer.

DISCUSSION

The circulating miRNAs are potential non-invasive biomarkers for diagnosis and prognostic prediction of cancer.[14,15] In this study, we identified an increased expression of miR-374a-5p in the serum of gastric cancer patients. The diagnostic value of serum miR-374a-5p was higher than traditional diagnostic markers, such as alpha fetoprotein (AFP) or carcino-embryonic antigen (CEA).[16] In addition, we found that the expression of miR-374a-5p was increased in the serum of patients with pre-cancerous gastric lesions, which was consistent with our previous study showing that the expression of miR-374a-5p was also increased in the serum of MNNG-exposed rats with atypical hyperplasia in gastric tissues.[4] Thus, miR-374a-5p may serve as a potential biomarker for the early diagnosis of gastric cancer. Moreover, the expression of miR-374a-5p decreased after surgical treatment, which suggests that miR-374a-5p may also be a good prognostic indicator. The expression of miR-374a-5p was increased in the serum of patients with relapse after oxaliplatin treatment and

Figure 2. miR-374a-5p Confers the Resistance of Gastric Cancer Cells to Oxaliplatin *In Vitro* and *In Vivo*

(A) CCK-8 assay for IC_{50} of mock, negative control, and miR-374a-5p mimic-transfected HGC-27 cells to oxaliplatin. (B and C) The mRNA and protein levels of MDR and Topo II were detected by qRT-PCR (B) and western blot (C). (D) Flow cytometric analyses of cell apoptosis in control and miR-374a-5p-transfected HGC-27 cells that were exposed to oxaliplatin for 48 h. (E) The size of tumors at the end of the experiment from mice treated with PBS + PBS, oxaliplatin + PBS, oxaliplatin + agomir negative control, and oxaliplatin + agomir-374a-5p. (F) Tumor growth curves in mice treated as indicated. The arrow refers to the oxaliplatin treatment initiated when tumors reached a volume of 50–100 mm^3. (G) The mean weight of tumors at the end of the experiment (at day 7 after chemotherapy treatment). (H) Immunohistochemical analyses of MDR and Topo II proteins in tumor tissues. Original magnification, ×200. Scale bars, 50 μm. (I) The apoptotic cells in tumor tissues were detected by TUNEL assay. Original magnification, ×200. Scale bar, 50 μm. *$p < 0.05$; **$p < 0.01$; ***$p < 0.001$.

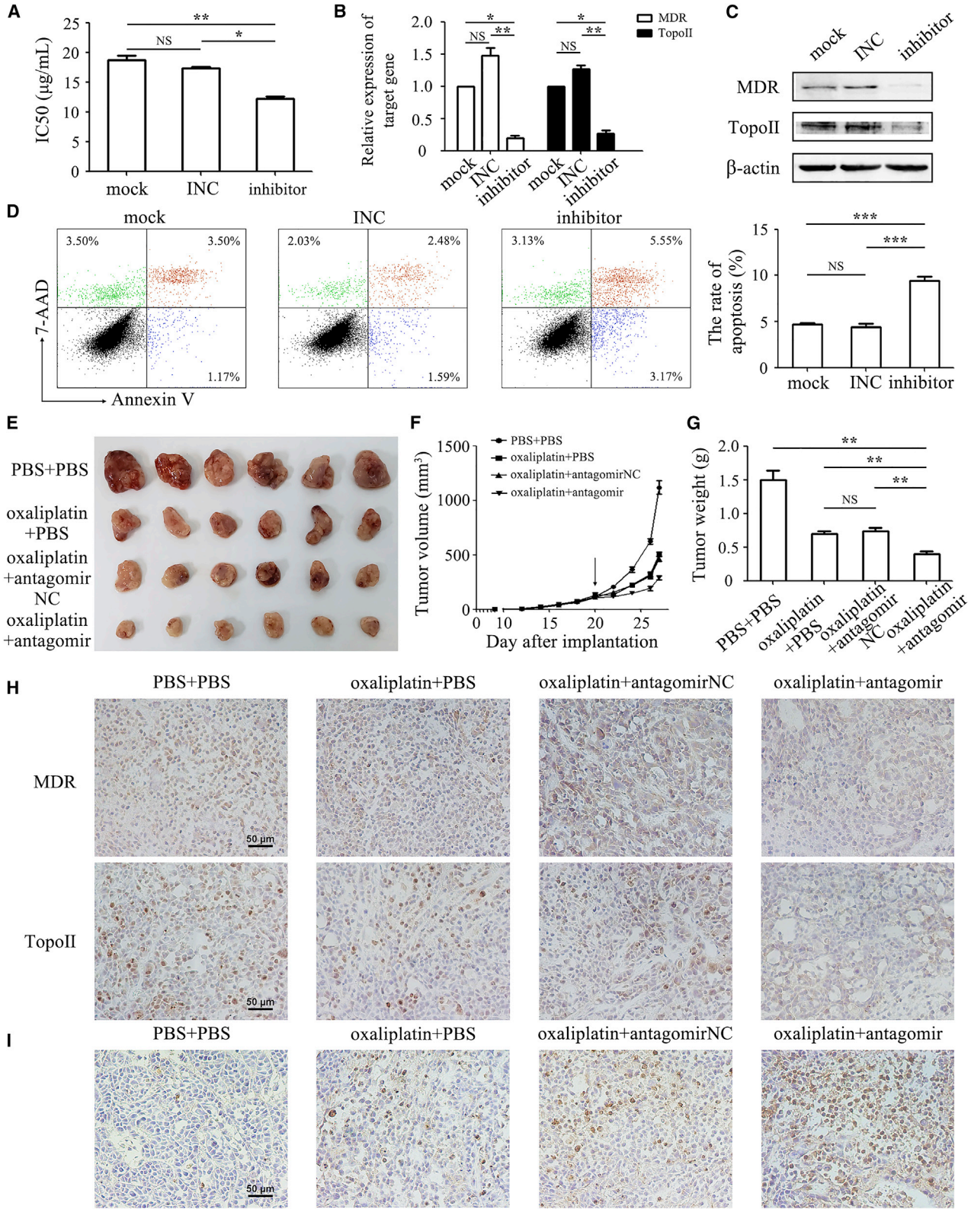

(legend on next page)

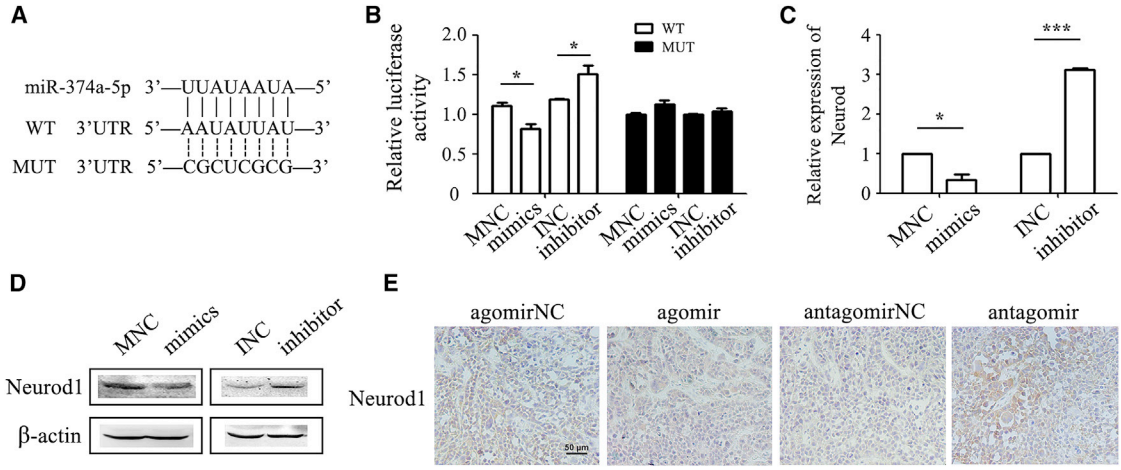

Figure 4. Neurod1 Is a Target of miR-374a-5p

(A) The predicted binding sites for miR-374a-5p in the 3′ UTR of Neurod1. WT, wild-type; MUT, mutant. (B) Luciferase activity in HGC-27 cells or oxaliplatin-HGC-27 cells that was transfected with wild-type or mutant reporter vectors and miR-374a-5p mimics or inhibitors. (C and D) The mRNA and protein levels of Neurod1 in HGC-27 cells transfected with miR-374a-5p mimics and oxaliplatin-HGC-27 cells transfected with miR-374a-5p inhibitors were detected by qRT-PCR (C) and western blot (D). (E) Immunohistochemical staining of Neurod1 in tumor tissues. *$p < 0.05$; ***$p < 0.001$.

oxaliplatin-resistant gastric cancer cells, indicating that miR-374a-5p plays an important role in the resistance of gastric cancer to chemotherapy.

We further demonstrated that miR-374a-5p enhanced the resistance of gastric cancer cells to oxaliplatin through Neurod1 *in vitro* and *in vivo*. Therefore, the downregulation of miR-374a-5p may be a novel approach to enhance the sensitivity of gastric cancer cells to chemotherapy. We first demonstrated that the inhibition of miR-374a-5p into gastric cancer cells could increase their sensitivity to oxaliplatin. We next proved that exosome-mediated delivery of anti-miR-374a-5p could re-sensitize gastric cancer cells to oxaliplatin by decreasing the expression of multidrug resistance proteins and promoting cell apoptosis. More importantly, exo-anti-374a-5p could decrease the chemoresistance of gastric cancer cells to oxaliplatin *in vivo*, indicating that miR-374a-5p may be an effective target for overcoming drug resistance in gastric cancer and exosomes may provide a new tool for delivering therapeutic inhibitor.

The importance of miRNAs in cancer chemotherapy has been demonstrated in many studies.[17] For example, miR-197 and miR-130b conferred cisplatin resistance in non-small-cell lung cancer by targeting the signal transducer and activator of transcription 3 (STAT3) and Wnt/β-catenin pathways.[18,19] In contrast, miR-125a-5p was able to reverse cisplatin resistance in esophageal squamous cell carcinoma by reducing the levels of STAT3.[20] miR-374b-5p was found to be dramatically decreased in pancreatic cancer tissues compared with adjacent normal tissues, as well as in a cisplatin-resistant pancreatic cancer cells. The downregulated miR-374b enhanced the chemosensitivity of cancer cells by modulating apoptotic pathways.[21,22] We found that the expression of miR-374a-5p was elevated in gastric cancer serum and in chemoresistant gastric cancer cells. The overexpression of miR-374a-5p promoted, while the silencing of miR-374a-5p abrogated the chemoresistance of gastric cancer cells to oxaliplatin *in vitro* and *in vivo*.

The basic helix-loop-helix (bHLH) transcription factor, neuronal differentiation 1 (Neurod1) (also known as BETA2) is involved in the development of neural elements and endocrine pancreas.[23] Diseases associated with Neurod1 include type 2 diabetes mellitus,[24] Alzheimer's disease,[25] and maturity-onset diabetes of the young 6 (MODY6).[26] However, its function in relation to cancer has been poorly examined. Studies proved that Neurod1 was related to neuroblastoma,[27] small-cell lung cancer,[28] and pancreatic cancer.[29] Here, we found Neurod1 might be involved in the drug resistance of gastric cancer.

Figure 3. Knockdown of miR-374a-5p Sensitizes Oxaliplatin-HGC-27 Cells to Oxaliplatin Treatment *In Vitro* and *In Vivo*

(A) CCK-8 assay for IC_{50} of oxaliplatin-HGC-27 cells with or without miR-374a-5p inhibitor transfection to oxaliplatin. Mock refers to untreated cells. INC refers to inhibitor negative control. (B and C) qRT-PCR (B) and western blot (C) for mRNA and protein expression of MDR and Topo II. (D) Flow cytometric analyses of cell apoptosis in oxaliplatin-HGC-27 cells with or without miR-374a-5p inhibitor transfection that were exposed to oxaliplatin for 48 h. (E) The size of tumors at the end of the experiment from mice treated with PBS + PBS, oxaliplatin + PBS, oxaliplatin + antagomir negative control, and oxaliplatin + antagomir-374a-5p. (F) Tumor growth curves in mice treated as indicated. The arrow refers to the oxaliplatin treatment initiated when tumors reached a volume of 50–100 mm^3. (G) The mean weight of tumors at the end of the experiment (at day 7 after chemotherapy treatment). (H) Immunohistochemical analyses of MDR and Topo II protein expression in tumor tissues. Original magnification, ×200. Scale bars, 50 μm. (I) Cell apoptosis in tumor tissues was detected by using TUNEL assay. Original magnification, ×200. Scale bar, 50 μm. *$p < 0.05$; **$p < 0.01$; ***$p < 0.001$.

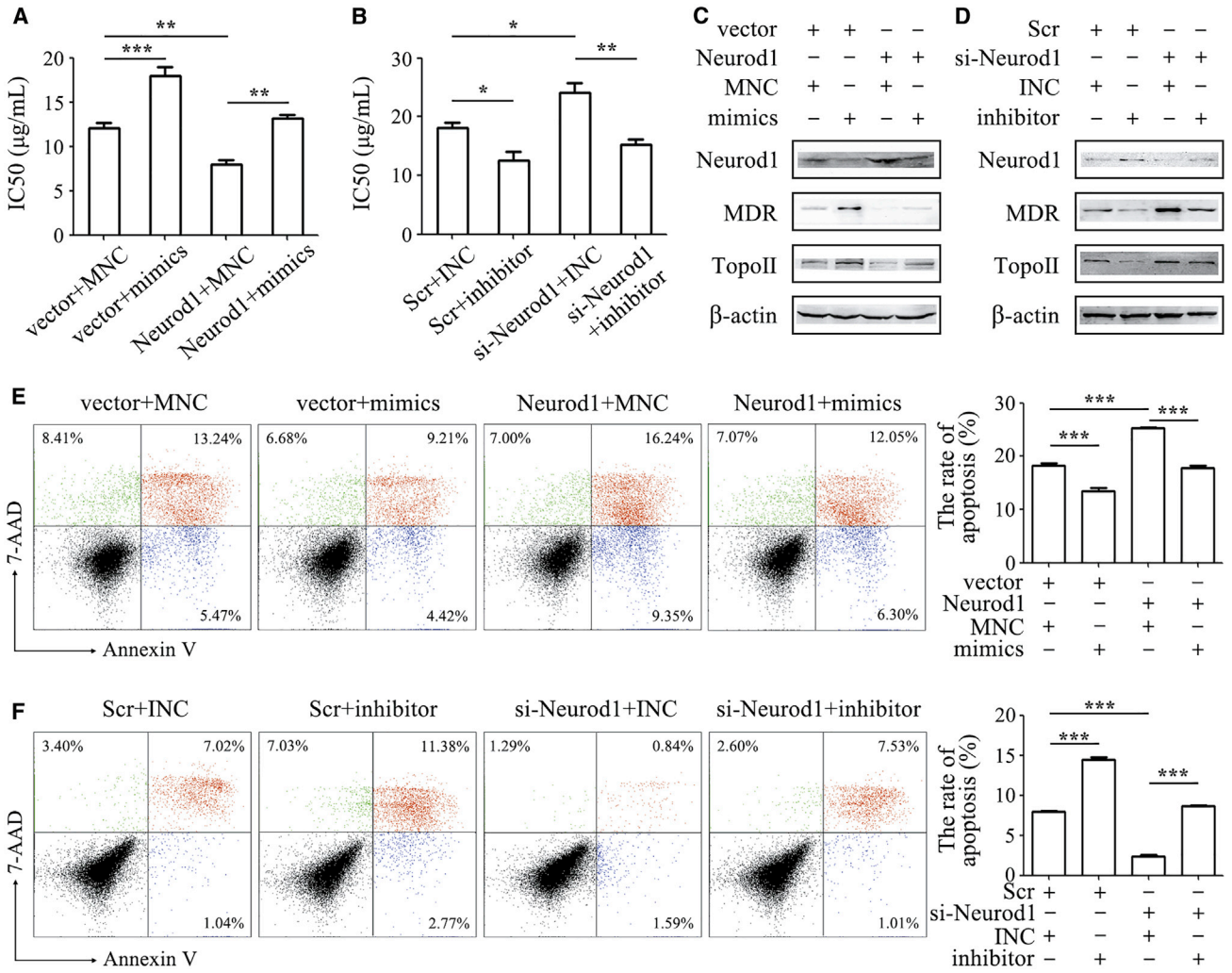

Figure 5. miR-374a-5p Reduces the Sensitivity of Gastric Cancer Cells to Oxaliplatin by Inhibiting Neurod1 Expression

HGC-27 or oxaliplatin-HGC-27 cells were transfected with miR-374a-5p mimics or inhibitors in the presence or absence of Neurod1 plasmid or si-Neurod1. (A and B) The IC_{50} of gastric cancer cells to oxaliplatin was determined by using CCK-8 assay in HGC-27 (A) and oxaliplatin-HGC-27 (B). (C and D) Western blot assay for the expression of MDR and Topo II proteins in HGC-27 (C) and oxaliplatin-HGC-27 (D). (E and F) Cell apoptosis was determined by using Annexin V/7-AAD double staining followed by flow cytometry analyses in HGC-27 (E) and oxaliplatin-HGC-27 (F). *$p < 0.05$; **$p < 0.01$; ***$p < 0.001$.

Exosomes have shown several advantages for cell-based gene therapy and nanomedicine. Exosomes could be conveniently stored and have high biocompatibility, which makes them ideal vehicles for gene or drug delivery. Exosomes derived from HEK293T cells have been suggested as reliable vehicles for the delivery of therapeutic molecules.[30] The previous study has shown that hepatocyte growth factor (HGF) siRNA transfected into HEK293T cells could be present in exosomes. The HGF siRNA-loaded exosomes suppressed the proliferation and migration of gastric cancer cells and inhibited tumor growth *in vivo*.[31] Exogenous anti-miR-214 within the exosomes is maintained at a stable level in the blood, which leads to the decreased expression of miR-214 in the tumors of mice, sensitizing the response of refractory gastric cancer to cisplatin.[32] Engineered exosomes derived from other donor cells have also been tested in cancer therapy. Exosomes from miR-122-modified adipose tissue-derived MSCs could increase the chemosensitivity of hepatocellular cancer.[33] Therefore, a comprehensive understanding of exosomes modification may provide a novel strategy for cancer therapy.

In conclusion, miR-374a-5p expression was elevated in patients with gastric cancer and could predict the therapy response of gastric cancer patients to chemotherapy. miR-374a-5p conferred drug resistance in gastric cancer by targeting Neurod1. Exosome-delivered anti-miR-374a-5p could re-sensitize gastric cancer cells to oxaliplatin. Our results suggest that miR-374a-5p is a new target for the diagnosis and drug resistance therapy of gastric cancer.

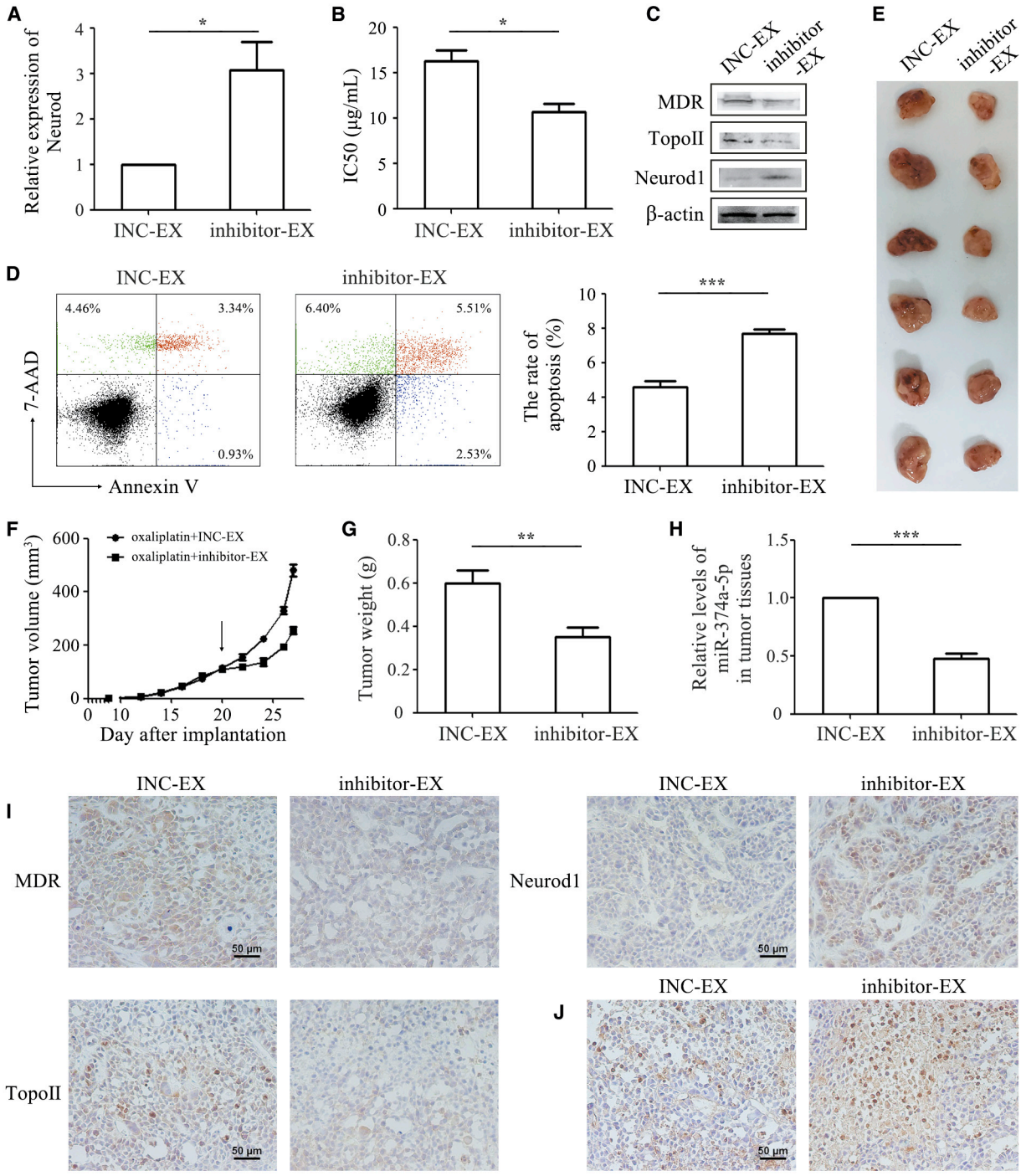

Figure 6. Exo-Anti-374a-5p Reverses the Resistance of Oxaliplatin-HGC-27 Cells to Oxaliplatin *In Vitro* and *In Vivo*

(A) The expression of Neurod1 in oxaliplatin-HGC-27 cells with or without exo-anti-374a-5p treatment was examined by using qRT-PCR. (B) CCK-8 assay was performed to determine the IC_{50} of oxaliplatin-HGC-27 cells with or without exo-anti-374a-5p treatment to oxaliplatin. (C) The expression of Neurod1, MDR, and Topo II proteins in oxaliplatin-HGC-27 cells with or without exo-anti-374a-5p treatment was determined by western blot. (D) The percentage of cell apoptosis in control and exo-anti-374a-5p-treated cells was tested by flow cytometry. (E) Images of tumors in mice in control and exo-anti-374a-5p-treated groups. (F and G) Tumor volumes (F) and tumor weights (G) in control and exo-anti-374a-5p-treated groups. (H) The expression levels of miR-374a-5p in tumors of control and exo-anti-374a-5p-treated groups were detected by qRT-PCR. (I) Immunohistochemical analyses of Neurod1, MDR, and Topo II protein expression in tumor tissues of control and exo-anti-374a-5p-treated groups. Original magnification, ×200. Scale bars, 50 μm. (J) Cell apoptosis in tumor tissues in control and exo-anti-374a-5p-treated groups was detected by using TUNEL assay. Original magnification, ×200. Scale bars, 50 μm. *$p < 0.05$; **$p < 0.01$; ***$p < 0.001$.

MATERIALS AND METHODS

Patients and Serum Samples

A total of 59 serum samples from gastric cancer patients, nine serum samples from patients of gastric cancer relapse after chemotherapy, five serum samples from patients with pre-cancerous lesions of gastric cancer, 17 serum samples from gastritis patients, and 17 serum samples from healthy donors were obtained from the Affiliated People's Hospital of Jiangsu University between November 2016 and May 2018. Written informed consent was obtained from all patients, and this study was approved by the Institutional Ethical Committee of Jiangsu University. The venous blood was centrifuged at 3000 × *g* for 10 min and the serum was stored at −80°C until miRNA extraction. The gastric cancer patients included in this study had not received any pre-operative therapies. The relapse patients all received oxaliplatin chemotherapy.

Cell Culture

Human gastric cancer cell lines MGC-803, SGC-7901, HGC-27, and HEK293T were purchased from the Cell Bank of the Chinese Academy of Sciences (Shanghai, China). MGC-803 and HEK293T cells were cultured in high-glucose DMEM (Wisent, Canada) with 10% fetal bovine serum (FBS; Thermo Fisher, USA). SGC-7901 and HGC-27 cells were cultured in RPMI 1640 medium (Wisent, Canada) containing 10% FBS. All the cells were cultured in a 37°C incubator with 5% CO_2 atmosphere. Oxaliplatin-resistant HGC-27 cells (oxaliplatin-HGC-27) were established by using the following procedure. After pre-treatment with 1 μg/mL of oxaliplatin for 48 h, the cells were changed to complete medium and cultured until growth recovery. The treatment was repeated for three cycles with increased doses of oxaliplatin, respectively (1, 3, 5 μg/mL).

Gene Overexpression and Silencing

miR-374a-5p inhibitor, inhibitor negative control (INC), miR-374a-5p mimics, mimic negative control (MNC), scramble control (Scr), Neurod1 siRNA, and overexpression plasmid (GenePharma, Shanghai, China) were transfected into the cells by using HiPerFect Transfection Reagent (QIAGEN, Germany) in serum-free medium. The concentration of inhibitor, mimics, siRNA, and plasmid was 200 nM, 30 nM, 100 nM, and 10 nM, respectively. Cells were changed to complete medium at 6 h after transfection and cultured for 48 h. Sequences and modifications of the oligonucleotides are shown in Table S1.

Cell Viability Assay

Cell viability was determined by using CCK-8 assay. HGC-27, MGC-803, SGC-7901, and oxaliplatin-HGC-27 cells with or without gene transfection were seeded in 96-well plates at 5×10^3 cells per well and incubated with oxaliplatin for 48 h. CCK-8 (10 μL per 100 μL) was added to each well for 1 h. The optical density was determined at 450 nm on a multi-well plate reader (FLX800, Bio-TEK). Background absorbance of the medium in the absence of cells was subtracted.

RNA Extraction and Quantitative Real-Time PCR

Total RNA was isolated from cells by using Trizol reagent (Thermo Fisher, USA). Total RNA in serum was purified by using an miRNeasy serum/plasma kit (QIAGEN, Germany) according to the manufacturer's procedures. Quantitative analyses of miRNA were performed with a miScript II RT kit and miScript SYBR green PCR kit (QIAGEN, Germany). Quantitative analyses of mRNAs were conducted with HiScript 1st strand cDNA synthesis kit and SYBR-green I real-time PCR kit (Vazyme, China) on a real-time PCR detection system (ABI 7500, Thermo Fisher). The relative expression levels of miRNAs and mRNAs were normalized to the expression of RNU6B and β-actin, respectively. miRNA primers were supplied by QIAGEN. All the primer sequences for mRNAs are listed in Table S2.

Western Blot

Cells were lysed with RIPA buffer (Merck Millipore, USA) containing protease inhibitors (Merck Millipore). Equal amounts of proteins were separated by SDS-PAGE on a 12% polyacrylamide gel. The proteins were transferred electrophoretically onto 0.22 μm polyvinylidene fluoride (PVDF) membranes (Merck Millipore), blocked in 5% non-fat milk, and then incubated with primary antibodies against MDR and topoisomerase II (Topo II) (Cell Signaling Technology, USA). β-actin (Cwbio, Beijing, China) was used as the loading control. After incubation with horseradish peroxidase (HRP)-linked secondary antibody, the protein bands were visualized by using chemiluminescence (Santa Clara, USA).

Luciferase Reporter Assay

HGC-27 or oxaliplatin-HGC-27 cells were co-transfected with miR-374a-5p mimics or inhibitor and the luciferase reporter vector containing WT or mutant (MUT) 3′ UTR of Neurod1 as indicated. At 48 h after transfection, the cells were lysed and the luciferase activity was detected by using the dual luciferase assay kit (Promega, Madison, WI, USA).

Cell Apoptosis Assay

Cells in early and late stages of apoptosis were detected by using an Annexin V-phycoerythrin (PE) apoptosis detection kit (BD Pharmingen, USA). Cells were exposed to oxaliplatin (3 μg/mL) for 48 h, collected, and analyzed in a Becton Dickinson FACS calibur instrument. Cells that were positive for Annexin V-PE alone (early apoptosis) and Annexin V-PE and 7-AAD (late apoptosis) were counted.

Isolation and Identification of Exosomes

The culture media from HEK293T cells transfected with or without miR-374a-5p inhibitor for 48 h were harvested and centrifuged at 2,000 × *g* to remove cell debris. Subsequently, the supernatant was centrifuged at 10,000 × *g* for 30 min to discard larger-sized shedding vesicles. After filtration by 100 kDa molecular weight cutoff (MWCO; Merck Millipore), the supernatant was incubated with ExoQuick (System Biosciences, SBI, USA) overnight. Exosomes in the precipitate were resuspended in PBS and filtered with 0.22-μm filters.

Transmission electron microscopy (TEM) and western blot for CD63, CD9 were performed to identify the isolated exosomes. The homogeneous exosome solution was dripped on the copper mesh and placed

at room temperature for 5 min. After sucking the residual liquid from the edge, the exosomes were dyed by 3% (w/v) phosphotungstic acid solution (pH 6.8) at room temperature for 5 min. The liquid was dried by incandescent lamp. Then the copper mesh was placed in the TEM sample room to observe the morphology of exosomes. The primary antibodies against CD9 and CD63 (Bioworld, USA) were used to detect exosomal markers by western blot. As for the absorption experiment of exosomes *in vitro*, exosomes labeled with chloromethyl-benzamidodialkylcarbocyanine (CM-Dil; red) at 37°C for 1 h were added into HGC-27 cells for 4 h. Cells were fixed and stained for cytoplasm (Cy2-actin, green) and nuclei (DAPI, blue). The fluorescence expression of cells were observed by laser confocal experiment.

Animal Model

Sixty female BALB/c nu/nu mice (Model Animal Research Center of Nanjing University, China), age 4 weeks, were randomly divided into 10 groups (n = 6). All groups received subcutaneous injections of HGC-27 cells or oxaliplatin-HGC-27 cells (3×10^6 cells in 200 μL PBS per mouse). Oxaliplatin was administered intraperitoneally (i.p.) at maximum tolerated dose level (10 mg/kg) when tumors reached a volume of 50-100 mm^3. Agomir-374a-5p, antagomir-374a-5p (2 optical density [OD] per mouse), and exosomes derived from miR-374a-5p inhibitor-transfected cells (exo-anti-374a-5p) (100 μg/mL) were administered intratumorally at the zeroth and the third day after oxaliplatin treatment, respectively. The mice were examined every 2 days since subcutaneous injection of tumor cells and sacrificed at the seventh day after oxaliplatin treatment. Tumor volumes were calculated by the modified ellipsoidal formula: $V = 1/2 (\text{length} \times \text{width}^2)$. All of the experimental procedures were performed according to protocols approved by the Animal Ethics Committee of Jiangsu University.

Immunohistochemistry

Formalin-fixed paraffin-embedded tissue sections were deparaffinized in xylene, rehydrated through graded ethanol, and then boiled for 10 min in citrate buffer (10 mM, pH 6.0) for antigen retrieval. Endogenous peroxidase activity was suppressed by exposure to 3% hydrogen peroxide for 10 min. Slides were then blocked with 5% BSA (Boster Bioengineering, Wuhan, China), incubated with primary antibodies against MDR and Topo II at 37°C for 1 h, and then incubated with secondary antibody at 37°C for 30 min. Slides were visualized with DAB (3,3′-diaminobenzidine) and counterstained with hematoxylin for microscopic examination.

TUNEL Staining

Apoptotic cells in tumor tissues were visualized by using the TUNEL assay. The TUNEL procedure was performed by using an *in situ* cell death detection kit (Boster, China) according to the manufacturer's instructions. The nuclei of apoptotic cells were dyed brown.

Statistical Analysis

All experiments were conducted at least in triplicate. Data were presented as means ± SD. Statistical analysis of the data was performed using SPSS22 software. Differences between groups were analyzed by Student's t test or one way ANOVA. A p value < 0.05 is considered to be significant.

SUPPLEMENTAL INFORMATION

Supplemental Information can be found online at https://doi.org/10.1016/j.omtn.2019.07.025.

AUTHOR CONTRIBUTIONS

R.J. performed the experimental work and drafted the manuscript. H.G., J.M., X.W., and J.Z. participated in the experiments; contributed reagents, materials, and analysis tools; and performed the statistical analysis. X.Z., H.Q., W.X., J.Q., and J.L. helped perform the analysis and participated in its design and coordination. X.Z. and J.L. revised the manuscript and approved the final version. All authors read and approved the final manuscript.

CONFLICTS OF INTEREST

The authors declare no competing interests.

ACKNOWLEDGMENTS

The present study was supported by the National Natural Science Foundation of China (grants 81702429 and 81672416), the Natural Science Foundation of the Jiangsu Province (grant BK20170561), and the Zhenjiang Science & Technology Program (grant SH2016047).

REFERENCES

1. Zhang, X., Liang, W., Liu, J., Zang, X., Gu, J., Pan, L., Shi, H., Fu, M., Huang, Z., Zhang, Y., et al. (2018). Long non-coding RNA UFC1 promotes gastric cancer progression by regulating miR-498/Lin28b. J. Exp. Clin. Cancer Res. *37*, 134.

2. Wang, M., Zhao, C., Shi, H., Zhang, B., Zhang, L., Zhang, X., Wang, S., Wu, X., Yang, T., Huang, F., et al. (2014). Deregulated microRNAs in gastric cancer tissue-derived mesenchymal stem cells: novel biomarkers and a mechanism for gastric cancer. Br. J. Cancer *110*, 1199–1210.

3. Sun, Z., Chen, J., Zhang, J., Ji, R., Xu, W., Zhang, X., and Qian, H. (2018). The role and mechanism of miR-374 regulating the malignant transformation of mesenchymal stem cells. Am. J. Transl. Res. *10*, 3224–3232.

4. Ji, R., Zhang, X., Qian, H., Gu, H., Sun, Z., Mao, F., Yan, Y., Chen, J., Liang, Z., and Xu, W. (2017). miR-374 mediates the malignant transformation of gastric cancer-associated mesenchymal stem cells in an experimental rat model. Oncol. Rep. *38*, 1473–1481.

5. Xie, J., Tan, Z.H., Tang, X., Mo, M.S., Liu, Y.P., Gan, R.L., Li, Y., Zhang, L., and Li, G.Q. (2014). MiR-374b-5p suppresses RECK expression and promotes gastric cancer cell invasion and metastasis. World J. Gastroenterol. *20*, 17439–17447.

6. Xu, X., Wang, W., Su, N., Zhu, X., Yao, J., Gao, W., Hu, Z., and Sun, Y. (2015). miR-374a promotes cell proliferation, migration and invasion by targeting SRCIN1 in gastric cancer. FEBS Lett. *589*, 407–413.

7. Venerito, M., Vasapolli, R., Rokkas, T., and Malfertheiner, P. (2018). Gastric cancer: epidemiology, prevention, and therapy. Helicobacter *23* (*Suppl 1*), e12518.

8. Stranford, D.M., and Leonard, J.N. (2017). Delivery of Biomolecules via Extracellular Vesicles: A Budding Therapeutic Strategy. Adv. Genet. *98*, 155–175.

9. Qiu, G., Zheng, G., Ge, M., Wang, J., Huang, R., Shu, Q., and Xu, J. (2018). Mesenchymal stem cell-derived extracellular vesicles affect disease outcomes via transfer of microRNAs. Stem Cell Res. Ther. *9*, 320.

10. Moradi-Chaleshtori, M., Hashemi, S.M., Soudi, S., Bandehpour, M., and Mohammadi-Yeganeh, S. (2019). Tumor-derived exosomal microRNAs and proteins as modulators of macrophage function. J. Cell. Physiol. *234*, 7970–7982.

11. Bunggulawa, E.J., Wang, W., Yin, T., Wang, N., Durkan, C., Wang, Y., and Wang, G. (2018). Recent advancements in the use of exosomes as drug delivery systems. J. Nanobiotechnology *16*, 81.

12. EL Andaloussi, S., Mäger, I., Breakefield, X.O., and Wood, M.J. (2013). Extracellular vesicles: biology and emerging therapeutic opportunities. Nat. Rev. Drug Discov. *12*, 347–357.

13. Pinheiro, A., Silva, A.M., Teixeira, J.H., Gonçalves, R.M., Almeida, M.I., Barbosa, M.A., and Santos, S.G. (2018). Extracellular vesicles: intelligent delivery strategies for therapeutic applications. J. Control. Release *289*, 56–69.

14. Link, A., and Kupcinskas, J. (2018). MicroRNAs as non-invasive diagnostic biomarkers for gastric cancer: Current insights and future perspectives. World J. Gastroenterol. *24*, 3313–3329.

15. Seijo, L.M., Peled, N., Ajona, D., Boeri, M., Field, J.K., Sozzi, G., Pio, R., Zulueta, J.J., Spira, A., Massion, P.P., et al. (2019). Biomarkers in lung cancer screening: achievements, promises and challenges. J. Thorac. Oncol. *14*, 343–357.

16. Reichl, P., and Mikulits, W. (2016). Accuracy of novel diagnostic biomarkers for hepatocellular carcinoma: An update for clinicians (Review). Oncol. Rep. *36*, 613–625.

17. Xie, M., Ma, L., Xu, T., Pan, Y., Wang, Q., Wei, Y., and Shu, Y. (2018). Potential Regulatory Roles of MicroRNAs and Long Noncoding RNAs in Anticancer Therapies. Mol. Ther. Nucleic Acids *13*, 233–243.

18. Fujita, Y., Yagishita, S., Hagiwara, K., Yoshioka, Y., Kosaka, N., Takeshita, F., Fujiwara, T., Tsuta, K., Nokihara, H., Tamura, T., et al. (2015). The clinical relevance of the miR-197/CKS1B/STAT3-mediated PD-L1 network in chemoresistant non-small-cell lung cancer. Mol. Ther. *23*, 717–727.

19. Zhang, Q., Zhang, B., Sun, L., Yan, Q., Zhang, Y., Zhang, Z., Su, Y., and Wang, C. (2018). MicroRNA-130b targets PTEN to induce resistance to cisplatin in lung cancer cells by activating Wnt/β-catenin pathway. Cell Biochem. Funct. *36*, 194–202.

20. Zhao, Y., Ma, K., Yang, S., Zhang, X., Wang, F., Zhang, X., Liu, H., and Fan, Q. (2018). MicroRNA-125a-5p enhances the sensitivity of esophageal squamous cell carcinoma cells to cisplatin by suppressing the activation of the STAT3 signaling pathway. Int. J. Oncol. *53*, 644–658.

21. Schreiber, R., Mezencev, R., Matyunina, L.V., and McDonald, J.F. (2016). Evidence for the role of microRNA 374b in acquired cisplatin resistance in pancreatic cancer cells. Cancer Gene Ther. *23*, 241–245.

22. Sun, D., Wang, X., Sui, G., Chen, S., Yu, M., and Zhang, P. (2018). Downregulation of miR-374b-5p promotes chemotherapeutic resistance in pancreatic cancer by upregulating multiple anti-apoptotic proteins. Int. J. Oncol. Published online March 14, 2018. https://doi.org/10.3892/ijo.2018.4315.

23. Demirbilek, H., Hatipoglu, N., Gul, U., Tatli, Z.U., Ellard, S., Flanagan, S.E., De Franco, E., and Kurtoglu, S. (2018). Permanent neonatal diabetes mellitus and neurological abnormalities due to a novel homozygous missense mutation in NEUROD1. Pediatr. Diabetes *19*, 898–904.

24. Mannino, G.C., and Sesti, G. (2012). Individualized therapy for type 2 diabetes: clinical implications of pharmacogenetic data. Mol. Diagn. Ther. *16*, 285–302.

25. Guo, Z., Zhang, L., Wu, Z., Chen, Y., Wang, F., and Chen, G. (2014). In vivo direct reprogramming of reactive glial cells into functional neurons after brain injury and in an Alzheimer's disease model. Cell Stem Cell *14*, 188–202.

26. Horikawa, Y., Enya, M., Mabe, H., Fukushima, K., Takubo, N., Ohashi, M., Ikeda, F., Hashimoto, K.I., Watada, H., and Takeda, J. (2018). NEUROD1-deficient diabetes (MODY6): Identification of the first cases in Japanese and the clinical features. Pediatr. Diabetes *19*, 236–242.

27. Huang, P., Kishida, S., Cao, D., Murakami-Tonami, Y., Mu, P., Nakaguro, M., Koide, N., Takeuchi, I., Onishi, A., and Kadomatsu, K. (2011). The neuronal differentiation factor NeuroD1 downregulates the neuronal repellent factor Slit2 expression and promotes cell motility and tumor formation of neuroblastoma. Cancer Res. *71*, 2938–2948.

28. Lehman, J.M., Hoeksema, M.D., Staub, J., Qian, J., Harris, B., Callison, J.C., Miao, J., Shi, C., Eisenberg, R., Chen, H., et al. (2019). Somatostatin receptor 2 signaling promotes growth and tumor survival in small-cell lung cancer. Int. J. Cancer *144*, 1104–1114.

29. Dugnani, E., Sordi, V., Pellegrini, S., Chimienti, R., Marzinotto, I., Pasquale, V., Liberati, D., Balzano, G., Doglioni, C., Reni, M., et al. (2018). Gene expression analysis of embryonic pancreas development master regulators and terminal cell fate markers in resected pancreatic cancer: A correlation with clinical outcome. Pancreatology *18*, 945–953.

30. You, B., Xu, W., and Zhang, B. (2018). Engineering exosomes: a new direction for anticancer treatment. Am. J. Cancer Res. *8*, 1332–1342.

31. Zhang, H., Wang, Y., Bai, M., Wang, J., Zhu, K., Liu, R., Ge, S., Li, J., Ning, T., Deng, T., et al. (2018). Exosomes serve as nanoparticles to suppress tumor growth and angiogenesis in gastric cancer by delivering hepatocyte growth factor siRNA. Cancer Sci. *109*, 629–641.

32. Wang, X., Zhang, H., Bai, M., Ning, T., Ge, S., Deng, T., Liu, R., Zhang, L., Ying, G., and Ba, Y. (2018). Exosomes Serve as Nanoparticles to Deliver Anti-miR-214 to Reverse Chemoresistance to Cisplatin in Gastric Cancer. Mol. Ther. *26*, 774–783.

33. Lou, G., Song, X., Yang, F., Wu, S., Wang, J., Chen, Z., and Liu, Y. (2015). Exosomes derived from miR-122-modified adipose tissue-derived MSCs increase chemosensitivity of hepatocellular carcinoma. J. Hematol. Oncol. *8*, 122.

OMTN, Volume *18*

Supplemental Information

miR-374a-5p: A New Target for Diagnosis and Drug Resistance Therapy in Gastric Cancer

Runbi Ji, Xu Zhang, Hongbing Gu, Jichun Ma, Xiangmei Wen, Jingdong Zhou, Hui Qian, Wenrong Xu, Jun Qian, and Jiang Lin

Supplementary Table 1. The sequences and modifications of the oligonucleotides.

Oligonucleotides	Sequences (5'-3')	Modifications
miR-374a-5p mimics	UUAUAAUACAACCUGAUAAGUG CUUAUCAGGUUGUAUUAUAAUU	"m" represents 2'-O-methyl-modified "s" represents phosphorothioate linkage "Chol" represents linked cholesterol
mimics NC	UUCUCCGAACGUGUCACGUTT ACGUGACACGUUCGGAGAATT	
miR-374a-5p inhibitors	mCmAmCmUmUmAmUmCmAmGmGmUmUmGmUmAmUmUmAmUmAmA	
inhibitors NC	mCmAmGmUmAmCmUmUmUmUmGmUmGmUmAmGmUmAmCmAmA	
Agomir-374a-5p	mU(s)m(s)UmAmUmAmAmUmAmCmAmAmCmCmUmGmAmUmAmA(s)mG(s)mU(s)mG(s)-Chol mC(s)mU(s)mUmAmUmCmAmGmGmUmUmGmUmAmUmUmAmUmA(s)mA(s)mU(s)mU(s)-Chol	
Agomir NC	mU(s)mU(s)mCmUmCmCmGmAmAmCmGmUmGmUmCmAmCmG(s)mU(s)mT(s)mT(s)-Chol	

	mA(s)mC(s)mGmUmGmAmCmAmCmGmUmUmCmGmGmAmGmA(s)mA(s)mT(s)mT(s)-Chol	
Antagomir-374a-5p	mC(s)mA(s)mCmUmUmAmUmCmAmGmGmUmUmGmUmAmUmUmA(s)mU(s)mA(s)mA(s)-Chol	
Antagomir NC	mC(s)mA(s)mGmUmAmCmUmUmUmUmGmUmGmUmAmGmUmA(s)mC(s)mA(s)mA(s)-Chol	
Si-Neurod1	GCAACUCAAUCCUCGGACUTT AGUCCGAGGAUUGAGUUGCTT	
Scr of si-Neurod1	UUCUCCGAACGUGUCACGUTT ACGUGACACGUUCGGAGAATT	

NC: negative control

Supplementary Table 2. Specific primers for target mRNAs.

Primers or oligonucleotides	Sequence (5' to 3')
H-MDR1-F	TCCTGGAGCGGTTCTACGAC
H-MDR1-R	GGCATGTATGTTGGCCTCCT
H-TopoII-F	GGCTTCCTGAGGATTACTTG
H- TopoII-R	GCCACTGATCCAGCTAATTG
H-Neurod-F	GCCACGACACGAGGAATT
H-Neurod-R	TCGCCCATCAGCCCACTCT
H-β-actin-F	CACGAAACTACCTTCAACTCC
H-β-actin-R	CATACTCCTGCTTGCTGATC

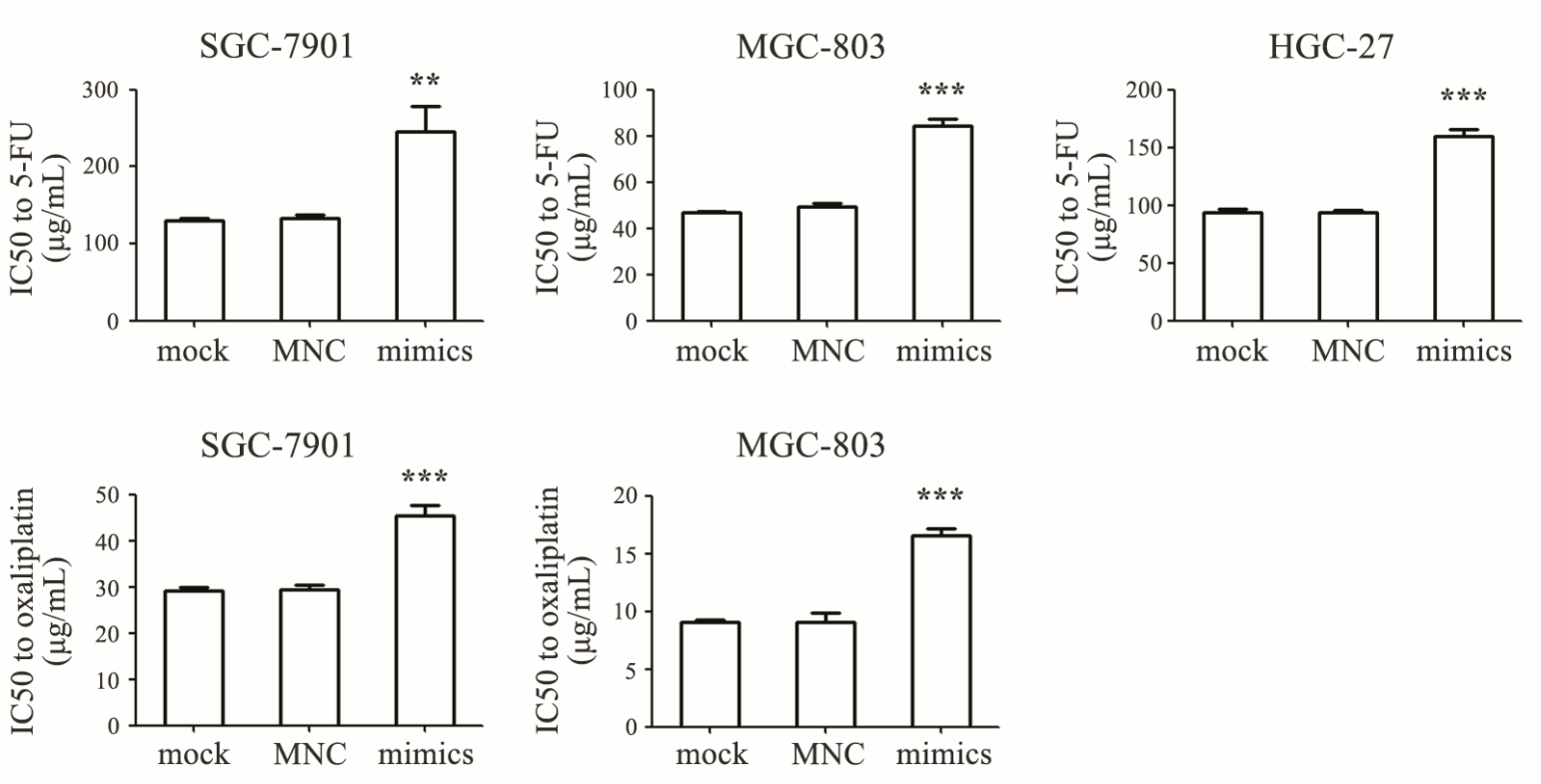

Supplementary Figure 1. MiR-374a-5p increased the IC50 of gastric cancer cells (HGC-27, MGC-803, and SGC-7901) to 5-FU and oxaliplatin.

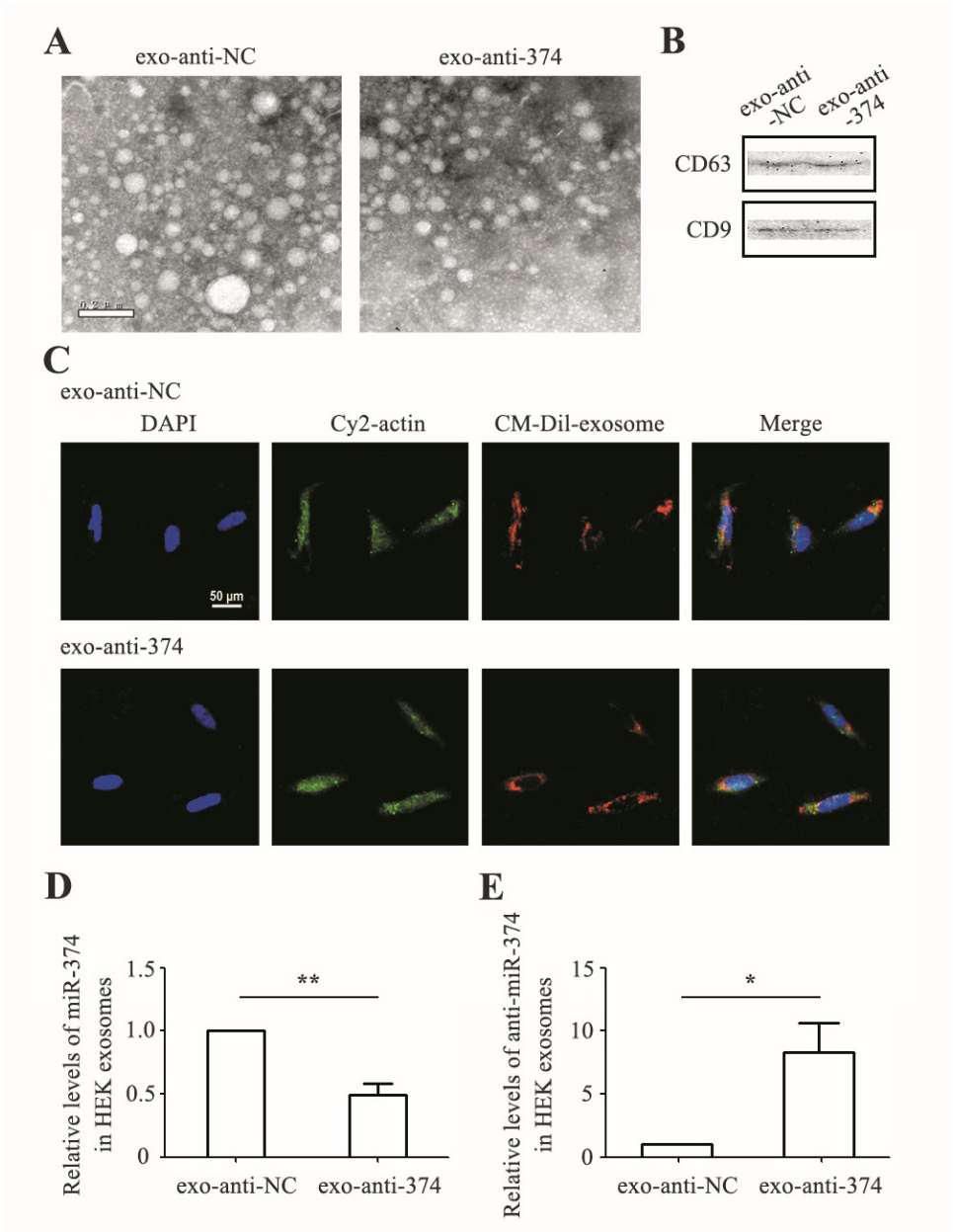

Supplementary Figure 2. The identification of exosomes and the expression of miR-374a-5p and miR-374a-5p inhibitor in exosomes. (A) The morphology of exosomes was observed by transmission electron microscope. Scale bar = 0.2 μm. (B) Western blot detected the expression of CD63 and CD9. (C) Internalization of exosomes into HGC-27 cells. Exosomes labeled with CM-Dil (red) at 37°C for 1 h were added into HGC-27 cells for 4 h. Cells were fixed and stained for cytoplasm (Cy2-actin, green) and nuclei (DAPI, blue). Original magnification, × 200. Scale bar = 50 μm. (D, E) The expression of miR-374a-5p and miR-374a-5p inhibitor in exosomes was determined by qRT-PCR.